Automation

International Edition: DOI: 10.1002/anie.201805632
German Edition: DOI: 10.1002/ange.201805632

A Fully Automated Continuous-Flow Platform for Fluorescence Quenching Studies and Stern–Volmer Analysis

*Koen P. L. Kuijpers[+], Cecilia Bottecchia[+], Dario Cambié, Koen Drummen, Niels J. König, and Timothy Noël**

Abstract: *Herein, we report the first fully automated continuous-flow platform for fluorescence quenching studies and Stern–Volmer analysis. All the components of the platform were automated and controlled by a self-written Python script. A user-friendly software allows even inexperienced operators to perform automated screening of novel quenchers or Stern–Volmer analysis, thus accelerating and facilitating both reaction discovery and mechanistic studies. The operational simplicity of our system affords a time and labor reduction over batch methods while increasing the accuracy and reproducibility of the data produced. Finally, the applicability of our platform is elucidated through relevant case studies.*

In the last decade, photoredox catalysis emerged as a powerful strategy for the catalytic activation of organic molecules.[1] In photoredox reactions, the ability of a photocatalyst to absorb visible light, reach an excited state and ultimately engage in a single electron transfer (SET) with an organic substrate is exploited as a powerful trigger to induce selective and unique transformations.[1a,2] In this context, a great deal of effort has been devoted to the understanding of the photophysical and photochemical aspects governing SET processes.[3] The translation of this knowledge to the field of organic synthesis has represented a key advantage in identifying novel photoredox transformations.[4]

Among the techniques employed to determine the reactivity of the excited state of a photocatalyst, fluorescence quenching studies occupy a prominent role. Once in their excited states, photocatalysts decay to their ground energy levels following either a radiative or non-radiative process (according to the kinetic constant k_0, which is a property of every chromophore).[3b] In other words, a photocatalyst dissipates the energy acquired through light absorption by either emitting light or heat. However, in presence of an organic molecule that can act as either energy acceptor or electron donor/acceptor, energy dissipation is averted and a productive transfer can occur, thus generating radical species of interest.[1a] Therefore, observing a decrease in the emission of an excited photocatalyst can be considered as a tangible proof of its interaction with an organic substrate and is the principle on which fluorescence quenching studies are based.[5]

To determine the rate at which an organic substrate can quench the excited state of a photocatalyst, a Stern–Volmer analysis can be conducted.[3b,6] In this case, the emission of a photocatalyst is measured at increasing concentration of the quencher.[7] However, despite their relevance in elucidating the interaction between organic substrates and photocatalysts, Stern–Volmer experiments are time-consuming and often air-sensitive. This is due to the fact that molecular oxygen is a known quencher of excited states, therefore a thorough Stern–Volmer analysis requires strictly inert conditions.[8] Moreover, because of the inevitable errors associated with human labor, the reproducibility and accuracy (R^2) of consecutive Stern–Volmer measurements is often problematic.[9] In addition, fluorescence quenching studies can also serve as a powerful tool to screen novel reactivities.[10] In order to facilitate, standardize and accelerate both quenching screening experiments and Stern–Volmer analysis, we envisioned an automated continuous-flow platform able to perform these analyses via in-line monitoring of the photocatalyst fluorescence (Scheme 1).

Recent reports demonstrated the implementation of automated platforms designed to assist chemists in the routine aspects of synthesis, leaving room for the intellectual pursuit of new chemical reactivities.[11] Bearing this prospect in mind, the automated platform we conceived minimizes the errors and the labor associated with fluorescence quenching experiments. Furthermore, our system has the potential to facilitate the way we perform these insightful experiments,

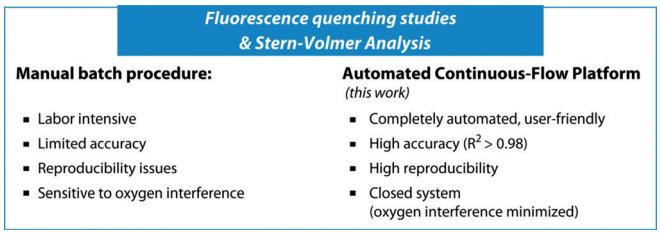

Scheme 1. Conceptual overview of the automated continuous-flow platform for fluorescence quenching studies and Stern–Volmer analysis.

[*] K. P. L. Kuijpers,[+] C. Bottecchia,[+] D. Cambié, K. Drummen, N. J. König, Dr. T. Noël
Department of Chemical Engineering and Chemistry, Sustainable Process Engineering, Micro Flow Chemistry & Process Technology, Eindhoven University of Technology
Den Dolech 2, 5612 AZ Eindhoven (The Netherlands)
E-mail: t.noel@tue.nl
Homepage: http://www.NoelResearchGroup.com
[+] These authors contributed equally to this work.
Supporting information and the ORCID identification number(s) for the author(s) of this article can be found under: https://doi.org/10.1002/anie.201805632.

thus offering a practical strategy for preliminary mechanistic investigations and accelerated reaction discovery in the context of photoredox catalysis.

When designing our system, we reasoned that continuous-flow technology would constitute a powerful mean to put into practice an automated platform for fluorescence quenching studies. Specifically, the confined dimensions of continuous-flow microreactors offer the advantage to minimize the volumes necessary for analysis and provide a closed environment that sustains inert conditions.[12] This aspect is especially relevant in light of the prohibitive costs of many photoredox catalysts.

An overview of the designed setup is depicted in Scheme 2. Continuous UV/Vis analysis of the catalyst fluorescence was achieved with a quartz flow cuvette (100 µL volume) connected through optical fibers to both a light source and a spectrophotometer with a 90° angle. Both the spectrophotometer and the light source are controlled by a computer. Moreover, dedicated HPLC pumps regulate the stream to the flow cuvette in an automated fashion.

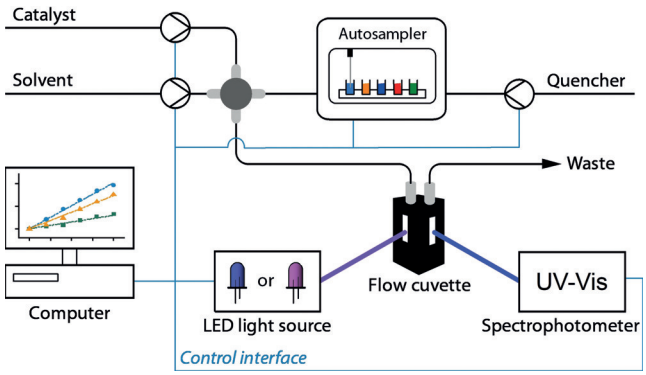

Scheme 2. Overview of the automated setup for fluorescence quenching studies and Stern–Volmer analysis.

Desiring to access a fully automated system suitable for both screening experiments and Stern–Volmer analysis, we focused on flexibility as the key property of our setup. The optimized setup can easily be operated in two modes: automated screening or Stern–Volmer analysis. When performing screening experiments, an autosampler is incorporated to inject all the samples to test in a solvent stream. This stream is then combined with a catalyst solution before entering the flow cuvette. When performing Stern–Volmer analysis, a third HPLC pump delivers the quencher solution, while the autosampler remains inactive. Another aspect further contributing to the flexibility of our system is the possibility to conveniently change LED light source in order to match the absorbance of the photocatalyst in use.

In both operational modes, all components were automated and controlled by a self-written Python script (the source code is freely available at GitHub).[13] The software features a user-friendly interface (see Supporting Information), which allows the user to easily fill in all experimental parameters without the need for any programming knowledge. All data collected during experiments are stored into an SQLite database, therefore progressively creating an easily accessible quencher library for known photocatalysts.

Our automated platform was first calibrated and tested with 9-mesityl-10-methyl acridinium perchlorate (Mes-Acr) as a model catalyst and with a series of amine quenchers (i.e. DIPEA, TMEDA, and TEA, Scheme 3).[14] The raw data set acquired via the in-line monitoring of the photocatalyst

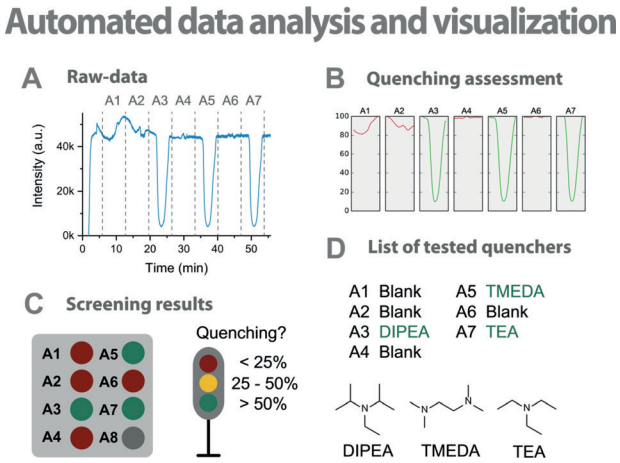

Scheme 3. Mes-Acr fluorescence quenching studies with a series of known amine quenchers. A) Raw-data from the spectrophotometer. B) Graphical output provided by the automated platform. C) Automated color-assignment of the tested quenchers and their meaning D) Tested quenchers.

fluorescence was automatically processed with a moving average function in order to minimize the fluctuations of the system (see SI, Section S4). Secondly, a time-based data extraction allowed us to cut the raw data set, thus minimizing storage space, facilitating data management and reducing the computing power necessary to generate a graphical output. Through data parsing, the software was then programmed to color-code the graphical peaks, each corresponding to the quenching degree of every quencher tested, in order to clearly identify the outcome of the screening test. Specifically, samples that afforded a quenching degree higher than 50% were assigned a green color, while yellow and red were chosen as colors for samples with a quenching degree between 50–25% and below 25% respectively (see SI, Section S4). Finally, the conclusions drawn from the quenching assessment can be analyzed by the user and converted to the results of the screening experiment, as exemplified in Scheme 3B and C.

We further dedicated our efforts to the automation of Stern–Volmer analysis. According to the Stern–Volmer relationship (Scheme 4), plotting the fraction of emission (i.e., photons emitted in absence of quencher over photons emitted in presence of quencher) against the concentration of quencher yields a linear relation, also known as Stern–Volmer plot (Scheme 4B).[3b] If the lifetime of the excited state (τ_0) of the photocatalyst is known, the quenching rate constant K_q can be derived from the slope of the Stern–Volmer plot.

We first conducted a Stern–Volmer analysis to determine the rate at which *N*,*N*,*N*′,*N*′-tetramethylethane-1,2-diamine

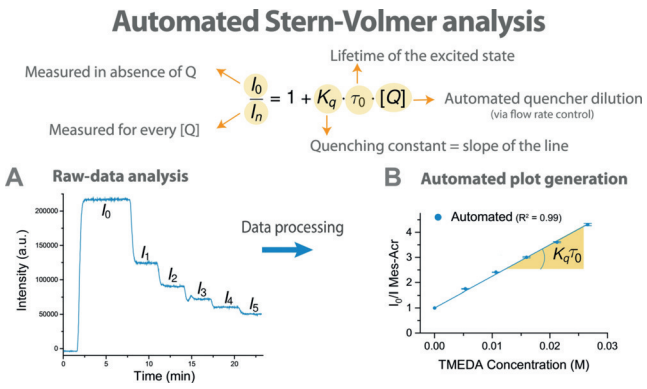

Scheme 4. Stern–Volmer equation and features of the automated measurement. A) Representation of the raw data for the quenching of Mes-Acr with increasing amounts of TMEDA. B) Automated plot generation.

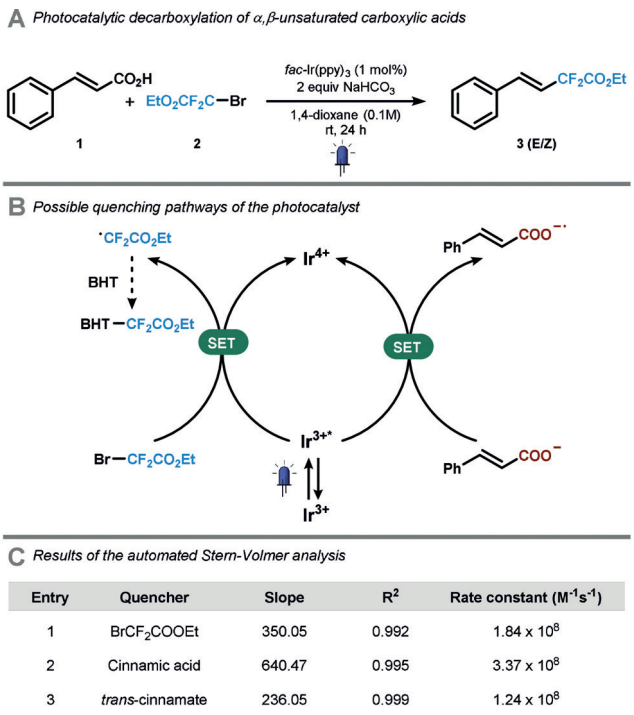

Entry	Quencher	Slope	R^2	Rate constant ($M^{-1}s^{-1}$)
1	$BrCF_2COOEt$	350.05	0.992	1.84×10^8
2	Cinnamic acid	640.47	0.995	3.37×10^8
3	*trans*-cinnamate	236.05	0.999	1.24×10^8

Scheme 5. A) Overview of the reaction conditions for the photocatalytic decarboxylation of α,β-unsaturated carboxylic acids. B) Possible first steps involved in the photocatalytic cycle. C) Results of the automated Stern–Volmer analysis.

(TMEDA) can quench the excited state of Mes-Acr. A representation of the raw data collected is shown in Scheme 4 A. The obtained ladder-like profile is consistent with the progressive decrease of emission intensity, which is in turn correlated with the injection of increasing concentrations of the quencher. We programmed the software to include the raw data into an Excel file and to automatically generate the corresponding Stern–Volmer plot (explicitly reporting the equation of the line and the R^2 value), thus relieving the user from this elementary task (Scheme 4 B). To showcase the reliability and the operational advantage that our automated platform offers, we performed multiple repetitions of the same Stern–Volmer analysis. As depicted in Scheme 4 B, ten consecutive experiments gave consistent results both in terms of accuracy (R^2) and reproducibility (for the precise slope value and quenching rate constant obtained, see SI). In this light, we believe that our system can be regarded as a convenient tool providing accurate, precise and reproducible results within a small time frame.

Moreover, it should be noted that despite the high quenching rate of molecular oxygen on the excited state of many commonly employed photocatalysts, the confined dimensions and the closed environment provided by our platform greatly contribute to reduce the impact of atmospheric oxygen on the measurements.[7]

With our automated platform in hand, we investigated its application in the elucidation of the first step involved in the mechanism of a photocatalytic reaction. We chose to investigate the $Ir(ppy)_3$-catalyzed photocatalytic decarboxylation of α,β-unsaturated carboxylic acids, a reaction developed in our laboratory (Scheme 5 A).[15] By comparing the excited state potentials of $Ir(ppy)_3$ ($E_{1/2}$ $Ir^{4+}/Ir^{*3+} = -1.73$ V and $E_{1/2}$ $Ir^{*3+}/Ir^{2+} = 0.31$ V vs. SCE) with the reduction potentials of $BrCF_2COOEt$ ($E_{red} = -0.57$ V vs. SCE, see SI) and cinnamic acid ($E_{red} = -1.09$ V vs. SCE, see SI), we reasoned that the reaction would most likely proceed through the oxidative quenching of the fluorinating agent, thus generating the CF_2COOEt radical of interest.[16] Nevertheless, due to the extremely high excited state oxidation potential of $Ir(ppy)_3$, we were curious to probe whether the reduction of cinnamic acid, albeit unexpected, could take place (Scheme 5 B). Thus, we performed a series of automated Stern–Volmer experiments to determine the rate at which ethyl bromodifluoroacetate or cinnamic acid can quench the excited state of $Ir(ppy)_3$. The results obtained are summarized in Scheme 5 C (for the Stern–Volmer plots see SI). To our surprise, our initial results showed a higher quenching rate constant for cinnamic acid compared to $BrCF_2COOEt$ (3.37×10^8 vs. 1.84×10^8 [$L\,mol^{-1}\,s^{-1}$]).

However, because of the fact that an excess of base is required in this reaction to generate *trans*-cinnamate, which is more prone to decarboxylation than its conjugate acid, we reasoned that the quenching rate of *trans*-cinnamate should be considered instead. The quenching rate constant of *trans*-cinnamate was found to be 1.24×10^8 [$L\,mol^{-1}\,s^{-1}$]. Thus, based on the slightly higher quenching rate constant obtained for $BrCF_2COOEt$, together with its higher concentration in the reaction mixture and its lower reduction potential, we propose that the first step involved in the photocatalytic cycle is most likely the oxidative quenching of $Ir(ppy)_3$ by $BrCF_2COOEt$. This hypothesis was further supported by the fact that a CF_2COOEt adduct was found when performing a radical trapping experiment with butylated hydroxytoluene (BHT). Notably, all the work required to confirm our initial mechanistic conclusion was performed by our automated system within less than an hour.

In a second case study, we became interested in the Ir-catalyzed decarboxylative alkylation of N-containing heteroarenes with *N*-(acyloxy)phthalimides (Scheme 6 A). Initially reported by Fu and co-workers, this reaction was found to proceed optimally when catalyzed by $Ir[dF(CF_3)ppy]_2$-

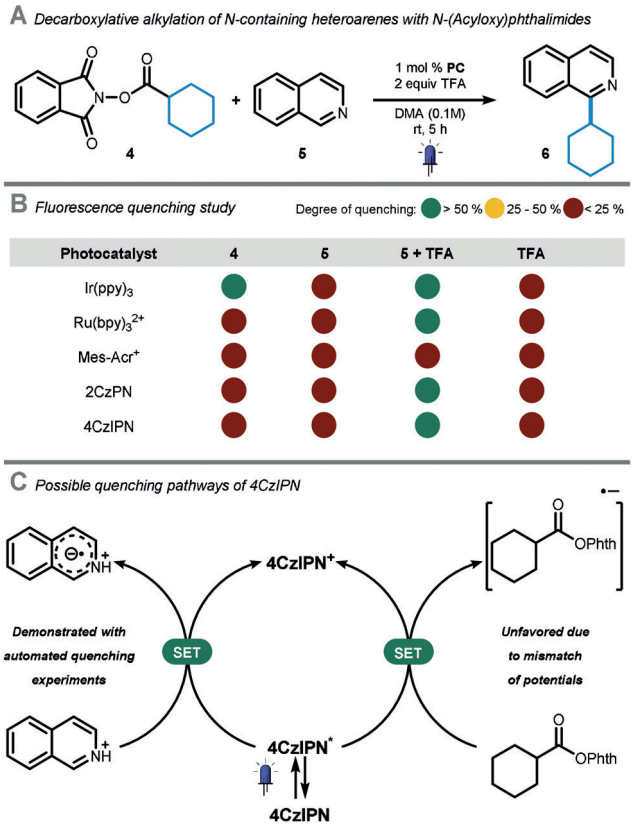

Scheme 6. A) Overview of the reaction conditions for the decarboxylative alkylation of N-containing heteroarenes with *N*-(Acyloxy)phthalimides. B) Results of the automated fluorescence quenching studies. C) Possible quenching pathways for the first mechanistic step.

(dtbbpy)PF_6 and in presence of an excess of strong acid (i.e., 2 equiv TFA).[17] Interested in replacing a costly iridium-based photocatalyst with an inexpensive alternative, we reasoned that a rapid photocatalyst screening performed with our automated platform would quickly present us with a viable substitute. A selection of catalysts to be tested was based on their absorption range and on their reported excited state potentials. Unaware of which catalytic cycle would be possible with the photocatalyst of choice, phthalimide **4**, isoquinoline **5** and isoquinoline **5** + TFA were tested as quenchers. As depicted in Scheme 6B, we found that no photocatalyst was quenched by phthalimide **4,** with the exception of $Ir(ppy)_3$.

These results seemed logical considering that $Ir(ppy)_3$ is the only photocatalyst with an excited state oxidation potential ($E_{1/2}$ $Ir^{4+}/Ir^{*3+} = -1.73$ V) sufficient for the direct reduction of phthalimide **4** ($E_{red} = -1.57$ V vs. SCE, see SI).[16] We also found that inexpensive organic photocatalysts 4CzIPN and 2CzPN both showed quenching in presence of protonated isoquinoline, while no quenching was observed with isoquinoline alone.[18] We rationalized these results by considering that, as documented in the literature, the protonation of isoquinoline **5** might result in a decrease of its reduction potential, thus rendering quenching with 4CzIPN and 2CzPN possible.[19] Naturally, both organic photocatalysts were then employed in the reaction of interest in a micro-capillary flow reactor, obtaining excellent isolated yields of the desired product **6** within 30 minutes of residence time (see SI).[12b] Finally, we conducted an automated Stern–Volmer analysis to determine the rate at which the protonated isoquinoline can quench the excited state of 4CzIPN and observed a quenching rate constant of 2.9×10^6 [$L\,mol^{-1}\,s^{-1}$] ($R^2 = 0.96$). Based on the results from the quenching studies, we suggest an oxidative quenching cycle in which protonated isoquinoline can quench the excited state of 4CzIPN (Scheme 6C).

In summary, we developed a fully automated continuous-flow platform for fluorescence quenching studies and Stern–Volmer analysis. The operational simplicity of our system reduces the time and labor associated with these analyses while increasing the accuracy and reproducibility of the data produced. We demonstrated the development, calibration, and application of our system to two case studies of interest. Ultimately, our automated platform has the potential to facilitate reaction discovery in photoredox catalysis. In this light, we believe that our automated continuous-flow platform will be of high interest both to a chemist and engineering audience and will inspire the design of similar machine-assisted screening systems.

Acknowledgements

Financial support was provided by a VIDI grant (SensPhotoFlow, 14150) and a Marie Curie ITN Grant (Photo4Future, 641861).

Conflict of interest

The authors declare no conflict of interest.

Keywords: automation · continuous flow · fluorescence quenching experiments · photoredox catalysis · Stern–Volmer

How to cite: *Angew. Chem. Int. Ed.* **2018**, *57*, 11278–11282
Angew. Chem. **2018**, *130*, 11448–11452

[1] a) C. K. Prier, D. A. Rankic, D. W. C. MacMillan, *Chem. Rev.* **2013**, *113*, 5322–5363; b) N. A. Romero, D. A. Nicewicz, *Chem. Rev.* **2016**, *116*, 10075–10166; c) E. C. Gentry, R. R. Knowles, *Acc. Chem. Res.* **2016**, *49*, 1546–1556.

[2] a) J. M. R. Narayanam, C. R. J. Stephenson, *Chem. Soc. Rev.* **2011**, *40*, 102–113; b) K. L. Skubi, T. R. Blum, T. P. Yoon, *Chem. Rev.* **2016**, *116*, 10035–10074.

[3] a) S. P. Pitre, C. D. McTiernan, J. C. Scaiano, *Acc. Chem. Res.* **2016**, *49*, 1320–1330; b) D. M. Arias-Rotondo, J. K. McCusker, *Chem. Soc. Rev.* **2016**, *45*, 5803–5820; c) V. Balzani, G. Bergamini, P. Ceroni, *Angew. Chem. Int. Ed.* **2015**, *54*, 11320–11337; *Angew. Chem.* **2015**, *127*, 11474–11492.

[4] a) E. R. Welin, C. Le, D. M. Arias-Rotondo, J. K. McCusker, D. W. C. MacMillan, *Science* **2017**, *355*, 380–385; b) J. C. Tellis, C. B. Kelly, D. N. Primer, M. Jouffroy, N. R. Patel, G. A. Molander, *Acc. Chem. Res.* **2016**, *49*, 1429–1439; c) M. A. Cismesia, T. P. Yoon, *Chem. Sci.* **2015**, *6*, 5426–5434; d) M. Marchini, G. Bergamini, P. G. Cozzi, P. Ceroni, V. Balzani,

Angew. Chem. Int. Ed. **2017**, *56*, 12820 – 12821; *Angew. Chem.* **2017**, *129*, 12996 – 12997; e) I. Ghosh, J. I. Bardagi, B. König, *Angew. Chem. Int. Ed.* **2017**, *56*, 12822 – 12824; *Angew. Chem.* **2017**, *129*, 12998 – 13000.

[5] J. R. Lakowicz, *Principles of Fluorescence Spectroscopy*, *Vol. 1*, Springer, Boston, **2006**.

[6] V. Balzani, G. Bergamini, P. Ceroni, *Rendiconti Lincei* **2017**, *28*, 125 – 142.

[7] S. P. Pitre, C. D. McTiernan, W. Vine, R. DiPucchio, M. Grenier, J. C. Scaiano, *Sci. Rep.* **2015**, *5*, 16397.

[8] H. Kautsky, *Trans. Faraday Soc.* **1939**, *35*, 216.

[9] M. R. Eftink, *Fluorescence Quenching: Theory and Applications*, *Vol. 2*, Springer, Boston, **2002**, pp. 53 – 126.

[10] a) M. N. Hopkinson, A. Gómez-Suárez, M. Teders, B. Sahoo, F. Glorius, *Angew. Chem. Int. Ed.* **2016**, *55*, 4361 – 4366; *Angew. Chem.* **2016**, *128*, 4434 – 4439; b) W. G. Lewis, F. G. Magallon, V. V. Fokin, M. G. Finn, *J. Am. Chem. Soc.* **2004**, *126*, 9152 – 9153; c) D. A. DiRocco, K. Dykstra, S. Krska, P. Vachal, D. V. Conway, M. Tudge, *Angew. Chem. Int. Ed.* **2014**, *53*, 4802 – 4806; *Angew. Chem.* **2014**, *126*, 4902 – 4906.

[11] a) H.-W. Hsieh, C. W. Coley, L. M. Baumgartner, K. F. Jensen, R. I. Robinson, *Org. Process Res. Dev.* **2018**, *22*, 542 – 550; b) C. W. Coley, M. Abolhasani, H. Lin, K. F. Jensen, *Angew. Chem. Int. Ed.* **2017**, *56*, 9847 – 9850; *Angew. Chem.* **2017**, *129*, 9979 – 9982; c) S. V. Ley, D. E. Fitzpatrick, R. M. Myers, C. Battilocchio, R. J. Ingham, *Angew. Chem. Int. Ed.* **2015**, *54*, 10122 – 10136; *Angew. Chem.* **2015**, *127*, 10260 – 10275; d) J. P. McMullen, M. T. Stone, S. L. Buchwald, K. F. Jensen, *Angew. Chem. Int. Ed.* **2010**, *49*, 7076 – 7080; *Angew. Chem.* **2010**, *122*, 7230 – 7234; e) F. Zhao, D. Cambie, V. Hessel, M. G. Debije, T. Noel, *Green Chem.* **2018**, *20*, 2459 – 2464; f) D. E. Fitzpatrick, C. Battilocchio, S. V. Ley, *ACS Cent. Sci.* **2016**, *2*, 131 – 138; g) B. J. Reizman, K. F. Jensen, *Acc. Chem. Res.* **2016**, *49*, 1786 – 1796; h) K. S. Elvira, X. C. i Solvas, R. C. R. Wootton, A. J. deMello, *Nat. Chem.* **2013**, *5*, 905 – 915.

[12] a) M. B. Plutschack, B. Pieber, K. Gilmore, P. H. Seeberger, *Chem. Rev.* **2017**, *117*, 11796 – 11893; b) D. Cambié, C. Bottecchia, N. J. W. Straathof, V. Hessel, T. Noël, *Chem. Rev.* **2016**, *116*, 10276 – 10341.

[13] K. P. L. Kuijpers, C. Bottecchia, D. Cambié, N. Konig, K. Drummen, T. Noel, **2017**, https://github.com/kkuijpers/Automated-quenching-studies.

[14] A. Joshi-Pangu, F. Lévesque, H. G. Roth, S. F. Oliver, L.-C. Campeau, D. Nicewicz, D. A. DiRocco, *J. Org. Chem.* **2016**, *81*, 7244 – 7249.

[15] X.-J. Wei, W. Boon, V. Hessel, T. Noël, *ACS Catal.* **2017**, *7*, 7136 – 7140.

[16] K. Teegardin, J. I. Day, J. Chan, J. Weaver, *Org. Process Res. Dev.* **2016**, *20*, 1156 – 1163.

[17] a) W.-M. Cheng, R. Shang, M.-C. Fu, Y. Fu, *Chem. Eur. J.* **2017**, *23*, 2537 – 2541; b) T. C. Sherwood, N. Li, A. N. Yazdani, T. G. M. Dhar, *J. Org. Chem.* **2018**, *83*, 3000 – 3012.

[18] a) J. Luo, J. Zhang, *ACS Catal.* **2016**, *6*, 873 – 877; b) H. Uoyama, K. Goushi, K. Shizu, H. Nomura, C. Adachi, *Nature* **2012**, *492*, 234 – 238.

[19] a) J. Zou, P. S. Mariano, *Photochem. Photobiol. Sci.* **2008**, *7*, 393; b) T. Damiano, D. Morton, A. Nelson, *Org. Biomol. Chem.* **2007**, *5*, 2735 – 2752; c) P. S. Mariano, *Tetrahedron* **1983**, *39*, 3845 – 3879.

Manuscript received: May 15, 2018
Accepted manuscript online: July 10, 2018
Version of record online: July 27, 2018

